

# Demonstration of Potential Benefits of Performance-Oriented Specifications

EMMANUEL G. FERNANDO AND ROBERT L. LYTTON

The implementation of performance-oriented specifications holds the promise of providing pavements that perform as they were designed to and of optimizing the use of tax dollars spent for highway construction. This will require the application of models relating materials, traffic, and environmental variables to expected pavement performance and life-cycle costs. To illustrate the potential benefits of performance-oriented specifications, hypothetical case studies were conducted in which the expected performance of pavements constructed using existing specifications was evaluated. The aim was to determine whether asphalts and mixtures considered to be acceptable under existing specifications may actually show significant differences in predicted performance and life-cycle costs under similar conditions, based on applications of the performance relationships selected for this particular exercise. The differences obtained would indicate the potential benefits of performance-oriented specification and the adequacy, or lack thereof, of existing specifications with respect to controlling asphalt and mixture properties that determine pavement performance.

Traditionally, state highway agencies have relied almost exclusively on recipe-type specifications for highway materials and construction. Under these specifications, the procedures to be followed in the construction of a pavement project are prescribed by the highway agency. A major drawback is that, by specifying materials, methods, and equipment, the highway agency obligates itself, to a great degree, to accept the end product, even though there is no assurance that it will meet the performance requirements.

More recently, many state highway agencies have adopted end-result specifications in which the contractor is given more latitude to choose construction methods and equipment and is responsible for controlling construction quality. Whereas these specifications are generally judged to be superior to traditional specifications, acceptance plans and price adjustment schedules are generally based on the historical ability of the producer or contractor to perform. Therefore, acceptance and payment tend to be based on current testing methods and construction practice rather than on test criteria and quality levels needed to achieve a certain level of performance.

Still another concept that has been introduced is that of performance-oriented specifications. The major difference between this type of specification and an end-result specification is that the acceptance plan and payment schedule are

tied to the predicted loss in pavement performance due to contractor nonconformance and to the resulting increase in pavement cost that will be incurred by the highway agency over the life of the project.

Performance-oriented specifications are a research item in the ongoing Strategic Highway Research Program (SHRP), which is expected to lead to the development of performance-based binder specifications. In addition, the recently completed NCHRP 10-26A project led to the development and demonstration of a conceptual framework for performance-related specifications for hot-mix asphalt concrete mixtures and to an identification of research needs to develop fully functional and reliable performance-related specifications (*1*).

The implementation of performance-oriented specifications promises to provide pavements that perform as they were designed to and to optimize the use of tax dollars spent for highway construction. To illustrate the potential benefits of performance-oriented specifications, hypothetical case studies were conducted in which the expected performance of pavements constructed using existing specifications was evaluated. The aim was to determine whether asphalts and mixtures considered to be acceptable under existing specifications may actually show significant differences in predicted performance and life-cycle costs under similar conditions, based on applications of the performance relationships selected for this particular exercise. The differences obtained would indicate the potential benefits of performance-oriented specifications and the adequacy, or lack thereof, of existing specifications with respect to controlling asphalt and mixture properties that determine pavement performance.

## CASE STUDIES

Three hypothetical case studies—designated as A, B, and C—were conducted to estimate the potential benefits of performance-oriented specifications

Case Study A involved the evaluation of the expected performance and life-cycle costs of two mixtures, prepared using the same asphalt, aggregates, and aggregate gradation but designed according to two different methods, referred to as Methods 1 and 2. Actual mix design data determined from laboratory tests were used.

Case Study B was conducted to estimate the effect of aggregate gradation on expected pavement performance and life-cycle costs. Two gradations were evaluated, as illustrated in Figure 1. In both cases, the gradations satisfy the ASTM grading specification for dense bituminous mixtures having a

E. G. Fernando, Texas Transportation Institute, Texas A&M University, College Station, Tex. 77843. R. L. Lytton, Department of Civil Engineering, Texas A&M University, College Station, Tex. 77843.

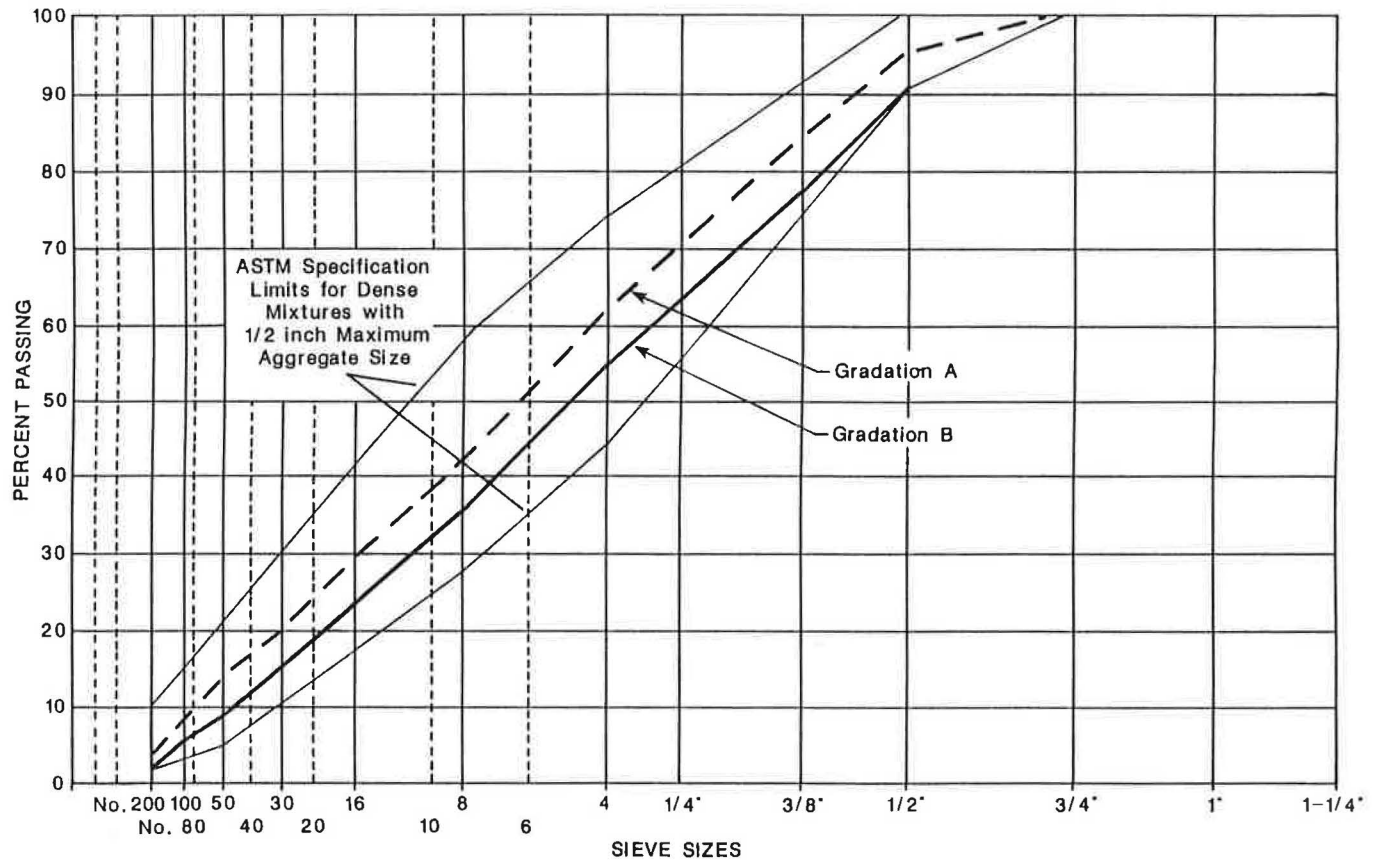


FIGURE 1 Aggregate gradations used for Case Study B.

nominal maximum aggregate size of  $\frac{1}{2}$  in. (ASTM D3515-89). For this case study, Jimenez's procedure (2) was used with the assumed gradations and assumed values of asphalt specific gravity, asphalt absorption, and effective specific gravity of the aggregate blend to predict theoretically the relationships between air voids, asphalt content, and film thickness for the two gradations evaluated.

Case Study C involved the evaluation of the expected performance and life-cycle costs of two mixtures, each prepared using a binder that meets the specifications for an AC-20 asphalt. The binders evaluated, designated as Binders 1 and 2, are included in the SHRP Materials Reference Library of asphalt cements. For this case study, bitumen stiffness data measured at different test temperatures and loading times were used in predicting pavement performance. Figures 2 and 3 illustrate the original bitumen stiffness data for the binders used in this case study.

## PERFORMANCE EVALUATION

The evaluation of expected pavement performance for the different case studies described generally followed a two-step procedure involving

1. The evaluation of fundamental material properties from basic mixture variables that are commonly used in existing specifications, such as asphalt content, air voids content, aggregate gradation, binder viscosity, and penetration; and

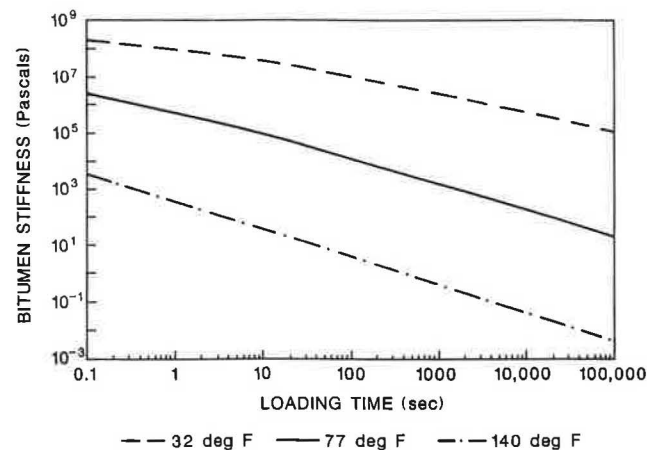


FIGURE 2 Original bitumen stiffness at various loading times and temperatures for Binder 1.

2. The application of existing performance models in conjunction with the fundamental material properties determined in Step 1 to predict fatigue cracking, rutting, and serviceability loss with time.

Two important fundamental material properties—the mixture stiffness and the slope of the creep compliance curve—were determined from the basic mixture data established for each case study. The relationship developed by Witczak was used to predict the dynamic modulus from data on volumetric

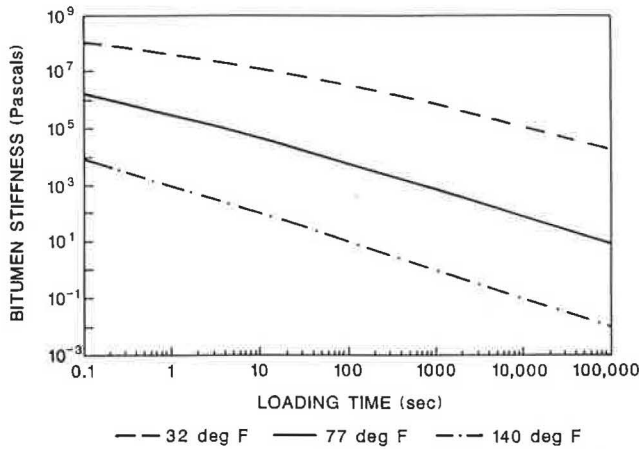


FIGURE 3 Original bitumen stiffness at various loading times and temperatures for Binder 2.

asphalt content, air voids content, aggregate gradation, and asphalt viscosity for each of the mixtures considered in Case Studies A and B (3). For Case Study C, McLeod's procedure was used with the available data on bitumen stiffness to estimate mixture stiffness. A computerized version of McLeod's nomograph was used for predicting the slope of the creep compliance curve for the three case studies (4).

The performance evaluation was made using a mechanistic finite element program called FLEXPASS developed at Texas A&M University. Because the results presented are dependent on the models used for predicting distress, the performance relationships in FLEXPASS are briefly described in the following. A detailed discussion of the development of FLEXPASS including efforts made to verify and calibrate the model is given by Tseng (5).

### Fatigue Cracking

The following phenomenological equation is used in FLEXPASS to predict fatigue cracking:

$$N_f = K_1 \left( \frac{1}{\epsilon_t} \right)^{K_2} \quad (1)$$

where

$N_f$  = number of load applications to failure,  
 $\epsilon_t$  = tensile strain at the bottom of the asphalt concrete layer, and

$K_1$  and  $K_2$  = fatigue parameters.

The fatigue parameters  $K_1$  and  $K_2$  of Equation 1 are evaluated in the FLEXPASS program using the following relationships derived by Tseng and Lytton (6) from fracture mechanics theory:

$$K_1 = \frac{d^{1-n/2} \left[ 1 - \left( \frac{C_o}{d} \right)^{1-nq} \right]}{[A(1-nq)(rE)^n]} \quad (2)$$

$$K_2 = n \quad (3)$$

where

$d$  = depth of the asphalt concrete layer,  
 $C_o$  = radius of the largest aggregate in the mix,  
 $E$  = mix stiffness,

$r$  and  $q$  = constants that relate the stress-intensity factor at the crack tip to the geometry of the sample, the loading, and the crack length, and

$A$  and  $n$  = fracture parameters of the Paris and Erdogan equation (7) given by

$$\frac{dc}{dN} = A(\Delta K)^n \quad (4)$$

where  $(dc)/(dN)$  is the rate of crack growth, and  $\Delta K$  is the change in the stress-intensity factor with each load cycle  $N$ .

On the basis of theoretical work done by Schapery (8) and experimental studies conducted at the Texas Transportation Institute (TTI), the following relationship for predicting the fracture parameter  $n$  was established (9).

$$n = 2/m \quad (5)$$

where  $m$  is the slope of the creep compliance curve.

Equation 5 is used, in conjunction with a computerized version of McLeod's nomograph to predict the fracture parameter  $n$ , thus the fatigue parameters  $K_1$  and  $K_2$  in the FLEXPASS program. The slope,  $m$ , of the creep compliance curve is estimated using McLeod's nomograph given the asphalt viscosity at 140 or 275°F, the penetration at 77°F, the asphalt content and air voids content of the mixture, and the service temperature. The fracture parameter  $A$  is estimated using the following regression equation developed from beam fatigue data:

$$\log_{10} A = 7.0889 - 2.4755n - 2.1163 \log_{10} E$$

$$R^2 = .86, N = 32 \text{ observations} \quad (6)$$

If the slope of the creep curve  $m$  and the fracture parameter  $n$  are known, the fatigue parameter  $K_2$  is determined. In addition, if the stiffness ( $E$ ) and the predicted value of  $n$  are known, the fracture parameter  $A$  can be estimated from Equation 6 and the fatigue parameter  $K_1$  can subsequently be predicted from Equation 2.

The fatigue parameters determined using this methodology are further adjusted to account for the healing of the pavement between load applications and residual stress buildup in the asphalt concrete layer. For this purpose, the predicted fatigue constants are adjusted following a procedure proposed by Tseng and Lytton (6).

After the parameters of the phenomenological equation for fatigue are determined, Miner's law is applied stochastically for predicting the increase in cracked area with time.

### Rutting Model

The increase in rut depth with time is predicted by accumulating the permanent vertical strains due to repetitive traffic loadings. In the procedure used, the permanent deformation

in each pavement layer is evaluated as the product of the total vertical resilient strain in a given layer and the fractional increase in total strain with cumulative load applications. The total vertical resilient strain is evaluated using the finite element method, whereas the fractional increase in total strain is predicted on the basis of an assumed model relating permanent strain to number of load repetitions. For the case studies conducted, the model used in the VESYS computer program (10) was adopted:

$$\varepsilon_a = IN^s \quad (7)$$

where

$$\begin{aligned} \varepsilon_a &= \text{permanent strain,} \\ N &= \text{cumulative load repetitions, and} \\ I \text{ and } s &= \text{model parameters determined from laboratory data.} \end{aligned}$$

Assuming that the resilient strain,  $\varepsilon_r$ , is large in comparison to the increase of permanent strain with each load repetition, the fractional increase in permanent strain is approximately given by

$$F(N) \approx \Delta\varepsilon_a/\varepsilon_r \quad (8)$$

where  $F(N)$  is the fractional increase in permanent strain with load repetition  $N$ .

The change in permanent strain,  $\Delta\varepsilon_a$ , is given by

$$\Delta\varepsilon_a = \frac{\partial\varepsilon_a}{\partial N} \quad (9)$$

Differentiating Equation 7 with respect to  $N$  and substituting the result into Equation 8 leads to the following expression for  $F(N)$ :

$$F(N) = \frac{ISN^{-(1-s)}}{\varepsilon_r} = \mu N^{-\alpha} \quad (10)$$

where  $\mu$  and  $\alpha$  are permanent deformation parameters. The rut depth,  $\delta_i(N)$ , for any given layer  $i$  is then determined by

$$\delta_i(N) = \int_0^N \int_0^{Z_{\max}} \varepsilon_c(Z) F(N) dZ dN \quad (11)$$

where

$$\begin{aligned} \delta_i(N) &= \text{rut depth at } N \text{ load repetitions for a layer } i, \\ Z_{\max} &= \text{depth of the pavement layer, and} \\ \varepsilon_c(Z) &= \text{vertical compressive strain at depth } Z. \end{aligned}$$

Finally, the total rut depth is obtained by adding the individual rut depths for each layer:

$$\begin{aligned} \delta(N) &= \sum_{i=1}^n \delta_i(N) = \sum_{i=1}^n \int_0^N \int_0^{d_i} \mu_i N^{-\alpha_i} dN \int_{d_{i-1}}^{d_i} \varepsilon_c(Z) dz \\ &= \sum_{i=1}^n \left\{ \frac{\mu_i}{1 - \alpha_i} N^{1 - \alpha_i} \int_{d_{i-1}}^{d_i} \varepsilon_c(Z) dz \right\} \end{aligned} \quad (12)$$

where

$$\begin{aligned} \delta_i(N) &= \text{total rut depth at } N \text{ load repetitions,} \\ n &= \text{number of pavement layers,} \\ d_{i-1} &= \text{depth at bottom of a layer } i, \text{ and} \\ d_i &= \text{depth at top of a layer } i. \end{aligned}$$

Equation 12 was used to predict the increase in rutting with cumulative load applications for the different case studies. In the analyses, the vertical compressive strain at a given depth within the layer was evaluated using the finite element method; the permanent deformation parameters ( $\alpha$  and  $\mu$ ) for the asphalt concrete layer were evaluated from the following relations:

$$\alpha = 1 - m \quad (13)$$

$$\mu = C_2(p)mt^m \quad (14)$$

where

$$\begin{aligned} C_2(p) &= \text{a calibration constant dependent upon the rutting characteristics of the asphalt mix and the quality of the aggregate,} \\ m &= \text{slope of the creep compliance curve, and} \\ t &= \text{time of loading.} \end{aligned}$$

Equation 13 is based on work done by Lytton (11), whereas Equation 14 is from development work conducted at TTI on the Texas Flexible Pavement System (12). For the base and subgrade layers, typical values for  $\alpha$  and  $\mu$  were assumed in the analyses and were kept the same for the three case studies.

### Serviceability Loss Model

With the FLEXPASS computer program, serviceability loss is evaluated using the AASHO present serviceability index (PSI) equation with the predicted values of rut depth, cracked area, and slope variance. The slope variance is predicted from the rut depth variance using the following equation based on VESYS (10):

$$E(SV) = \frac{2\beta}{c} \text{var}(\delta) \quad (15)$$

where

$$\begin{aligned} E(SV) &= \text{expected value of slope variance,} \\ \text{var}(\delta) &= \text{variance of rut depth, and} \\ \beta \text{ and } c &= \text{constants that have typical values of 1.0 and 0.058, respectively, based on regression analysis of field roughness data.} \end{aligned}$$

The rut-depth variance is evaluated from a probabilistic analysis of the rut-depth equation.

### Age-Hardening

In the analyses conducted, age-hardening of the different mixtures was also considered using relationships developed for

predicting the change in asphalt viscosity and penetration with time. These equations are based on data collected by Lee from eight different projects in Iowa, where observations of asphalt penetration and viscosity were made at 6-month intervals over 4 years (13). A hyperbolic model of the form given by Equation 16 was used to model the change in asphalt consistency with time.

$$\Delta y = t/(a + bt) \tag{16}$$

where  $\Delta y$  is the difference between the measured viscosity or penetration at time  $t$  and the value of the property at time of construction, and  $a$  and  $b$  are hyperbolic model parameters that are functions of basic mixture variables.

Relationships for predicting the hyperbolic model parameters of Equation 16 were developed and are summarized as follows:

• Viscosity at 70°F (megapoises):

$$a = 1.614494 \times 10^{-14} \cdot (V_{ref,70})^{3.1530} \cdot (FT)^{1.9937} \cdot (V_{140,TFOT})^{2.7830} \cdot (P_{air}/P_{200})^{-0.5283}$$

$$R^2 = .9963, RMSE = 0.0368, N = 8 \text{ obs.}$$

$$b = 6.0399 \cdot P_{ac}^{0.3322} \cdot (P_{30}/P_4)^{1.2935} \cdot (P_{air})^{-0.2102} \cdot (V_{140,TFOT}/V_{140,0})^{-0.8081}$$

$$R^2 = .9833, RMSE = 0.0186, N = 8 \text{ obs.}$$

• Viscosity at 140°F (poises):

$$a = 1.285740 \times 10^{-10} \cdot (V_{140,TFOT})^{2.1875} \cdot (P_{30}/P_4)^{-14.5233} \cdot (\text{pen}_{77,TFOT}/FT)^{-3.1502}$$

$$R^2 = .9619, RMSE = 0.1176, N = 8 \text{ obs.}$$

$$b = 0.2979 \cdot (P_8)^{-6.5466} \cdot (P_{30})^{11.8950} \cdot (P_{air})^{-2.2582} \cdot (\text{pen}_{77,TFOT}/FT)^{-4.0697}$$

$$R^2 = .9558, RMSE = 0.0746, N = 8 \text{ obs.}$$

• Penetration at 77°F (0.1 mm):

$$a = 3.287416 \times 10^{-5} \cdot (\text{pen}_{ref,77})^{-9.0932} \cdot (\text{pen}_{77,0})^{11.5555} \cdot (P_{200}/P_{30})^{4.2124}$$

$$R^2 = .9723, RMSE = 0.1192, N = 8 \text{ obs.}$$

$$b = 190,387 \cdot (FT)^{0.3245} \cdot (P_{air})^{-0.2860} \cdot (\text{pen}_{77,0})^{-4.0208} \cdot (P_{200}/P_{30})^{-1.2031} \cdot (\text{pen}_{77,TFOT}/\text{pen}_{77,0})^{-1.042}$$

$$R^2 = .9708, RMSE = 0.0144, N = 8 \text{ obs.}$$

where

$V_{ref,70}$  = reference viscosity at 70°F, at time of construction (megapoises);

- FT = film thickness (microns);
- $V_{140,TFOT}$  = viscosity at 140°F after thin-film oven testing (TFOT) (poises);
- $\text{pen}_{ref,77}$  = reference penetration at 77°F, at time of construction (0.1 mm);
- $\text{pen}_{77,TFOT}$  = penetration at 77°F after TFOT (0.1 mm);
- $\text{pen}_{77,0}$  = original penetration at 77°F (0.1 mm);
- $V_{140,0}$  = original viscosity at 140°F (poises);
- $P_{air}$  = percentage air voids;
- $P_{ac}$  = percentage asphalt;
- $P_{200}$  = percentage passing No. 200 sieve;
- $P_{30}$  = percentage passing No. 30 sieve;
- $P_8$  = percentage passing No. 8 sieve; and
- $P_4$  = percentage passing No. 4 sieve.

For viscosity, the dependent variable  $\Delta y$  in Equation 16 is  $\log_{10}(V_t/V_{ref})$ , where  $V_t$  is the predicted viscosity at time  $t$  and  $V_{ref}$  is the reference viscosity. For penetration,  $\Delta y$  is the predicted difference between the reference penetration, and the penetration at some time  $t$ . In both cases, the reference values should be the estimated properties at the time of construction.

The preceding equations were used to estimate the effects of aging on the predicted performance of the different mixtures evaluated in Case Studies A and B. The prediction equations for viscosity at 70°F were used in conjunction with the dynamic modulus equation developed by Witczak to predict the change in modulus with time (3). The equations for viscosity at 140°F and penetration at 77°F were used to predict the change in fatigue and permanent deformation properties as the mixture ages. Table 1 summarizes the data used in conjunction with the given equations to evaluate the age-hardening of the mixtures considered in Case Studies A and B. For Case Study C, estimates of bitumen stiffness with time, obtained from a SHRP A-002 subcontractor, were used in conjunction with McLeod's procedure (4) to predict the change in mixture stiffness with time.

The predicted age-hardening characteristics of the different mixtures were used in subdividing the analysis period into several time intervals, with each time interval characterized by mixture properties representative of the aging associated with the given interval. A 20-year analysis period was used

TABLE 1 Input Data Used to Characterize Age-Hardening for Case Studies A and B

Input Variable	Case Study A		Case Study B	
	Method 1	Method 2	Gradation A	Gradation B
1. $V_{ref,70}$ (megapoises)	17.55	17.55	17.55	17.55
2. FT (microns)	9.92	10.97	8.52	13.76
3. $V_{140,TFOT}$ (poises)	2637	2637	2637	2637
4. $V_{140,0}$ (poises)	1071	1071	1071	1071
5. $\text{pen}_{ref,77}$ (0.1 mm)	38	38	38	38
6. $\text{pen}_{77,TFOT}$ (0.1 mm)	51	51	51	51
7. $\text{pen}_{77,0}$ (0.1 mm)	85	85	85	85
8. $P_{air}$ (%)	4.9	3.9	4	4
9. $P_{ac}$ (%)	5.4	5.9	4.73	5.18
10. $P_{200}$ (%)	3.9	3.9	3.9	2.0
11. $P_{30}$ (%)	20.2	20.2	20.2	15.2
12. $P_8$ (%)	41.8	41.8	41.8	35.8
13. $P_4$ (%)	61.6	61.6	61.6	54.6

for all case studies. The performance evaluation for each mixture was therefore conducted in stages, starting with the first time interval and proceeding in succession through the last time interval or period. At each time period, the associated mixture properties were used in conjunction with the selected performance models to predict the fatigue cracking, rutting, and serviceability loss for that particular period. The predicted levels of distress at the end of any given time period were then used as the starting levels of distress for the subsequent time period.

### LIFE-CYCLE COST ANALYSIS

For all case studies, a hypothetical pavement section consisting of a 4 in. bituminous-bound surface layer and a 10 in. granular base course overlaying a clay subgrade was assumed. A 9,000-lb load acting on dual wheels spaced 13 in. apart and inflated to a pressure of 75 psi was used to represent the standard 18-kip equivalent single axle load (ESAL). In addition, an initial traffic rate of 353 ESALs a day and a traffic growth rate of 4 percent were used in the simulations. The cumulative traffic for the 20-year analysis period was approximately 4 million 18-kip ESALs.

Properties of the surface layer were varied depending on the particular bituminous mixture that was being evaluated. These properties varied with time and with the assumed seasonal temperatures. For all mixtures, the properties of the base and the subgrade layers were kept the same.

The performance predictions were used in evaluating the life-cycle costs for the different case studies considered. For this analysis, the following failure criteria were used to determine the timing of overlays:

1. Maximum allowable fatigue cracking—500 ft<sup>2</sup>/1,000 ft<sup>2</sup>.
2. Maximum allowable rut depth—0.50 in.
3. Terminal serviceability index—2.50.

An overlay was assumed to be necessary when one or more of these failure limits has been reached. For the life-cycle cost analysis, the thickness design of overlays was accomplished using the overlay design equations developed for FHWA (14). These equations assume that overlay life is governed by reflection cracking. For each case study, an overlay thickness was determined to last the remainder of the analysis period. The properties of the overlay material for determining the required overlay thicknesses were kept the same for all three case studies.

Life-cycle costs were calculated using a cost-analysis program known as FLAGCAP developed at TTI in a recent research project sponsored by the Florida Department of Transportation (15). Pavement costs associated with the predicted performance of each of the different mixtures were evaluated, and included costs due to initial construction, routine maintenance, overlays, and level-ups. In addition, user costs associated with vehicle depreciation, fuel consumption, oil consumption, tire wear, vehicle maintenance, and user travel time were estimated on the basis of assumed distribution of vehicles in the traffic stream and the predicted serviceability history for the given analysis period. The assumed vehicle distribution was compatible with the daily 18-kip ESALs

used in the performance evaluation. In addition, user operating costs were adjusted for the effects of pavement roughness using relationships developed from data compiled by Zaniewski (16).

Future costs were converted to equivalent present worth costs using a discount rate of 5 percent. A summary of the pavement and user costs evaluated for the different case studies considered is presented in Table 2. The costs shown are for a 10-mi stretch of one-lane roadway; they are specific to the case studies considered herein.

As may be observed from Table 2, the percent difference in pavement costs associated with the different case studies considered varies from approximately 3.9 to 12.5 percent. Considering that the mixtures in each case study are, by existing specifications, "equally acceptable," the differences in pavement life-cycle costs obtained illustrate the need for specifications that are based on predicted pavement performance, and indicate the potential savings that may be realized if such specifications are implemented. Note that the predicted pavement costs shown in Table 2 are only for a 10-mi stretch of one-lane highway. If the predicted differences in pavement costs are applied over an entire highway network, the potential savings can easily be substantial and will be even more if the potential reductions in user costs are also considered. This is readily apparent from Table 2, in which it is observed that the predicted differences in user costs are significantly greater than the predicted differences in pavement costs. This indicates that not only will highway agencies realize savings from implementing performance-oriented specifications, but that road users will, as well, and at a potentially greater amount.

### ILLUSTRATION OF ALTERNATIVE APPROACH TO SPECIFICATION DEVELOPMENT

The limited number of simulations conducted therefore demonstrate the importance of developing materials and construction specifications on the basis of predicted pavement performance. This will entail specifications on variables that significantly influence pavement service life. The choice of variables to be controlled will logically depend on the distress criteria and models used for pavement design, which in turn may vary with local conditions. Whatever materials and construction variables are selected for specification purposes, the choice should be guided by the following considerations: (a) the variables selected are significant predictors of pavement performance, and (b) the variables are properties that can be controlled by the producer or contractor during construction.

The first guideline can be addressed through a sensitivity analysis of the particular distress prediction models used in pavement design. By way of illustration, the slope  $m$  of the creep compliance curve is a material property input to the simulation program, FLEXPASS, used in different hypothetical case studies considered herein. How this material property relates to expected pavement performance is evident from the mechanics-based relationships presented earlier between the slope of the creep curve, the fatigue parameters, and the permanent deformation parameters. To illustrate the sensitivity of the performance predictions from FLEXPASS to variations in the slope of the creep curve, simulation runs were made wherein the slope was varied from 0.40 to 0.50

**TABLE 2 Summary of Life-Cycle Costs for Three Case Studies**

Speculative Case Study	Time to Failure (Years)	Failure Mode	Pavement Cost (x 1000\$)	Difference in Pavement Costs (x 1000\$)	Percent Difference in Pavement Cost	User Cost (x 1000\$)	Difference in User Costs (x 1000\$)	Total Cost (x 1000\$)	Difference in Total Costs (x 1000\$)
<b>A. Mix Design Method</b>									
1. Method 1	6.55	Fatigue Cracking	765			437,825		438,590	
2. Method 2	5.59	Rutting	796	31	3.89	438,325	500	439,121	531
<b>B. Effect of Aggregate Gradation</b>									
1. Gradation A	12.27	Fatigue Cracking	679			430,703		431,382	
2. Gradation B	7.34	Fatigue Cracking	740	61	8.24	436,525	5,822	437,265	5,883
<b>C. Viscosity Grading</b>									
1. Binder 1	12.24	Fatigue Cracking	765			425,901		426,666	
2. Binder 2	8.52	Fatigue Cracking	874	109	12.47	428,118	2,217	428,992	2,326

and all other variables were held constant. The layer thicknesses and base and subgrade properties from earlier runs were also used in these new simulations. Figures 4, 5, and 6 illustrate the performance predictions obtained.

Based on the distress models used, it is apparent from the figures that the slope ( $m$ ) of the creep curve is a significant predictor of pavement performance. Life-cycle costs associated with the different levels of this material property are summarized in Table 3, which indicates substantial differences in predicted pavement life-cycle costs between the cases considered. These results further demonstrate the importance of the slope of the creep curve, and how, from a performance prediction standpoint, it is an appropriate variable to use for establishing target values for construction quality control. An example of how this may be done is illustrated in Figure 7 and Table 4. Assuming for instance a required minimum predicted service life of 20 years and a required maximum pre-

dicted pavement life-cycle cost of \$10,000/lane-mi, a target value of 0.40 for the slope ( $m$ ) of the creep curve is obtained based on the results of simulations. This target value is of course specific to the conditions analyzed and will undoubtedly vary depending on traffic and environmental conditions and with different pavement layer thicknesses and material properties. The effect of deviations from target on predicted pavement life-cycle costs will then be used as the basis for establishing payment schedules in a performance-based specification.

**CONCLUSION**

On the basis of the hypothetical case studies reported herein, it is apparent that existing asphalt and mixture specifications do not necessarily ensure that pavements constructed "within

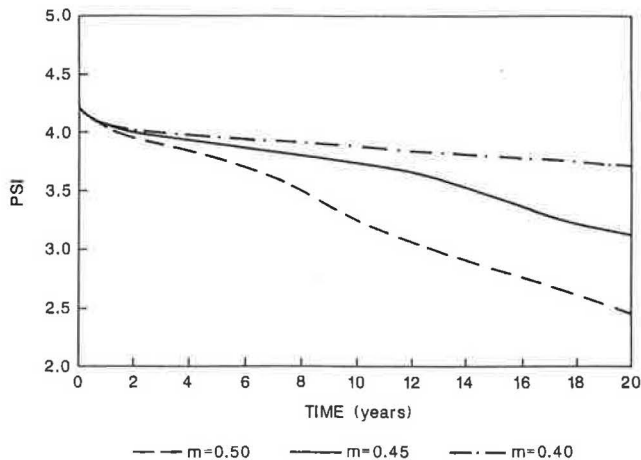


**FIGURE 4 Predicted trends in serviceability loss with time for different levels of  $m$ .**

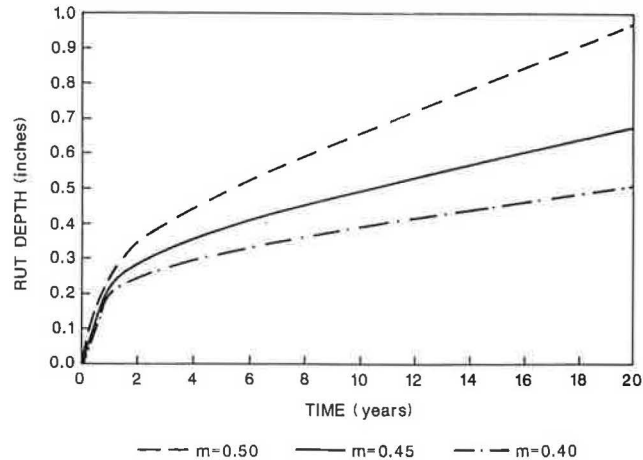


**FIGURE 5 Predicted trends in rutting with time for different levels of  $m$ .**

specs" will yield similar performance and life-cycle costs. Indeed, the simulations have shown that significant differences in pavement life-cycle costs may be predicted for asphalt mixtures that are within specification limits. Consequently, there is merit to implementing specifications that are tied to predicted pavement performance.

As part of developing performance-oriented specifications, materials and construction variables have to be identified which are significant predictors of pavement performance and are factors that can be controlled during construction. The choice of materials and construction variables for specification development will logically depend on the distress criteria and models used for pavement design. An example of a material property for which target values for construction quality control may be specified is the slope of the creep compliance curve. This material property has been shown, from theory, to be a predictor of fatigue cracking and rutting, and its significance as a performance-related variable was illustrated herein.

It is emphasized that the slope ( $m$ ) was only used as an example of the kinds of materials and construction variables that need to be considered for specification development. Fundamental material properties such as the slope of the creep curve or mixture stiffness may be suitable variables to use from the standpoint of being performance-related, but implementing working specifications based on these variables is another issue. It is recognized that actual measurement of fundamental material properties for determining compliance to specifications may be beyond existing capabilities of some state highway agencies and contractors. For this reason, sur-

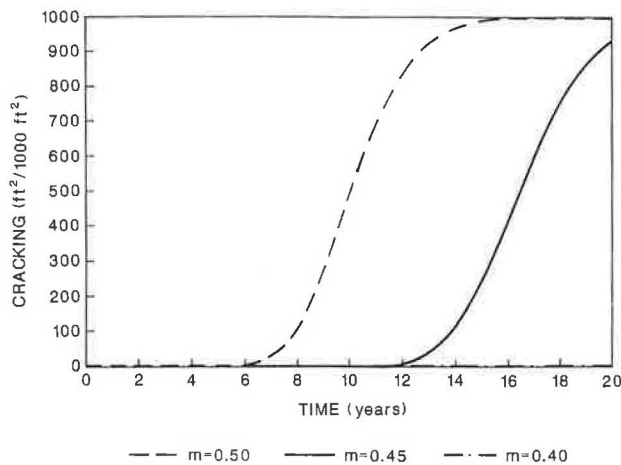


FIGURE 6 Predicted trends in fatigue cracking with time for different levels of  $m$ .

TABLE 3 Summary of Life-Cycle Costs for Different Values of  $m$

SLOPE, $m$ , OF CREEP CURVE	PAVEMENT COST <sup>a</sup> (x 1000 \$)	DIFFERENCE IN PAVEMENT COSTS (x 1000) <sup>b</sup>	USER COST <sup>a</sup> (x 1000 \$)	DIFFERENCE IN USER COST (x 1000) <sup>b</sup>
0.50	566	---	231,157	---
0.45	387	-179	227,448	-3,709
0.40	87	-479	220,818	-10,339

<sup>a</sup> Present worth costs for a 10-mile, one lane stretch of highway; 20-yr analysis period at a 5% discount rate.

<sup>b</sup> Relative to costs for case where slope  $m = 0.50$ .

PERFORMANCE CRITERIA:

LIFE  $\geq$  20 Years

$$\frac{\text{Agency Cost} \leq \$10,000}{\text{Lane Mile}} \leq \frac{\text{Life Cycle Cost}}{\text{Lane Mile}}$$

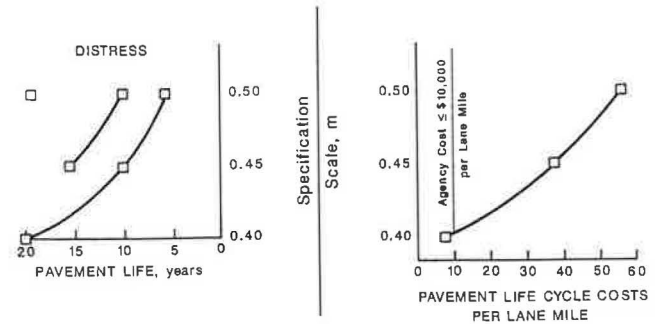


FIGURE 7 Determination of target value for  $m = 0.40$  based on performance considerations.

TABLE 4 Failure Time (Years) for Figure 7

Slope, $m$	Distress			Agency Life Cycle Costs per Lane Mile (x \$1000)
	PSI (2.5)*	Rutting (0.5 in)*	Fatigue (600ft <sup>2</sup> /1000ft <sup>2</sup> )*	
0.40	—	20	—	8.7
0.45	—	10	17	38.7
0.50	19	5.43	10	56.6

\*Failure Criterion

rogate tests or relationships for these variables may have to be used that relate fundamental material properties, which are significant predictors of pavement performance, to materials and construction variables that have been traditionally used in materials and construction specifications. Alternatively, algorithms may be developed, or existing procedures implemented, for estimating fundamental material properties in situ. Already, there are a number of computer programs available for back calculation of layer stiffnesses from measured surface deflections, including a recent computer program called SCALPOT, developed by Magnuson and Lytton at Texas A&M University (17), that is capable of estimating creep compliance parameters of layered systems from falling weight deflection measurements. Developments like these should provide additional impetus for acceptance and implementation of performance-oriented specifications within the highway community.

REFERENCES

1. D. A. Anderson et al. *Performance-Related Specification for Hot-Mix Asphaltic Concrete*. Final Report, NCHRP 10-26A. Pennsylvania Transportation Institute, Pennsylvania State University, University Park, Aug. 1990.
2. R. A. Jimenez and D. A. Dadeppo. *Asphalt Concrete Mix Design*. Report ATTI-86-2. Arizona Transportation and Traffic Institute, University of Arizona, Tucson, June 1986.
3. M. W. Witzczak. *The Universal Airport Pavement Design System—Report II: Asphaltic Mixture Material Characterization*. University of Maryland, College Park, May 1989.
4. N. W. McLeod. Asphalt Cements: Pen-Vis Number and Its Application to Moduli Stiffness. *Journal of Testing and Evaluation*, Vol. 4, No. 4, 1976.



5. K. Tseng. *A Finite Element Method for the Performance Analysis of Flexible Pavements*. Ph.D. dissertation. Texas A&M University, College Station, 1988.
6. K. Tseng and R. L. Lytton. Fatigue Damage Properties of Asphaltic Concrete Pavements. In *Transportation Research Record 1286*, TRB, National Research Council, Washington, D.C., 1990.
7. P. C. Paris and F. Erdogan. A Critical Analysis of Crack Propagation Laws. *Journal of Basic Engineering* (Transactions of the ASME, Series D), Vol. 85, No. 3, 1963.
8. R. A. Schapery. A Theory of Crack Growth in Viscoelastic Media. Technical Report MM.2764-73-1. Mechanics and Materials Research Center, Texas A&M University, College Station, 1973.
9. F. P. Germann and R. L. Lytton. *Methodology for Predicting the Reflection Cracking Life of an Overlay*. Report TTI-2-8-75-207-5. Texas Transportation Institute, Texas A&M University, College Station, March 1979.
10. W. J. Kenis. Predictive Design Procedures—A Design Method for Flexible Pavements Using the VESYS Structural Subsystem. *Proc., 4th International Conference on the Structural Design of Asphalt Pavements*, Vol. 1, University of Michigan, Ann Arbor, 1977, pp. 101–138.
11. R. L. Lytton. Materials Property Relationships for Modeling the Behavior of Asphalt-Aggregate Mixtures in Pavements. Technical Memorandum SHRP A-005. Strategic Highway Research Program, Washington, D.C., June 1990.
12. J. Uzan, D. G. Zollinger, and R. L. Lytton. *The Texas Flexible Pavement System (TFPS), Volume II—Mechanistic/Empirical Model*. Research Report 455-1. Texas Transportation Institute, Texas A&M University, College Station, Nov. 1990.
13. D. Lee. Asphalt Durability Correlation in Iowa. In *Highway Research Record 468*, HRB, National Research Council, Washington, D.C., 1973, pp. 43–60.
14. P. W. Jayawickrama, R. E. Smith, R. L. Lytton, and M. R. Tirado. *Development of Asphalt Concrete Overlay Design Equations: Volume I—Development of Design Procedures*. Final Report DTFH61-84-C-00053. FHWA, McLean Va., 1987.
15. E. G. Fernando, R. L. Lytton, W. L. McFarland, J. L. Memmott, F. Helin, and A. N. Jamy. *The Florida Comprehensive Pavement Analysis System (COMPAS)—Volume I: Development of Analytical Models*. Texas Transportation Institute, Texas A&M University, College Station, April 1991.
16. J. P. Zaniewski, B. C. Butler, G. Cunningham, G. E. Elkins, M. S. Paggi, and R. Machemehl. *Vehicle Operating Costs, Fuel Consumption, and Pavement Type and Condition Factors*. Report DOT-FH-11-9678. U.S. Department of Transportation, June 1982.
17. A. H. Magnuson, R. L. Lytton, and R. C. Briggs. A Comparison Study of Computer Predictions and Field Data for Dynamic Analysis of Falling Weight Deflectometer Data. Presented at the 70th Annual Meeting of the Transportation Research Board, Washington, D.C., Jan. 1991.

---

*The contents of this paper reflect the views of the authors, who are responsible for the facts and accuracy of the evaluation presented herein. The contents do not necessarily reflect the official views or policies of TRB or FHWA.*